Programmed Synthesis of Copolymer with Controlled Chain Composition Distribution via Semibatch RAFT Copolymerization

Xiaoying Sun,[†,‡] Yingwu Luo,*[,†] Rui Wang,[†] Bo-Geng Li,*[,†] Bei Liu,[†] and Shiping Zhu*[,§]

Department of Chemical and Biochemical Engineering, State Key Laboratory of Polymer Reaction Engineering, Zhejiang University, Hangzhou 310017, P.R. China, School of Biological and Chemical Engineering, Zhejiang University of Science and Technology, Hangzhou 310012, P.R. China, Department of Chemical Engineering, McMaster University, Hamilton, Ontario, Canada L8S 4L7

Received July 25, 2006; Revised Manuscript Received December 2, 2006

ABSTRACT: It is well-known that controlled/living radical copolymerization (CLRcoP) yields gradient copolymer with the composition varying along chain length. The composition distribution of the as-synthesized product is solely determined by the comonomer reactivity ratios and is thus not well controlled. This work reports the first experimental example of the control over the copolymer composition distribution through semibatch operations. Using styrene (St)/butyl acrylate (BA) as a model system, we synthesized uniform and linear gradient copolymers via semibatch reverse addition−fragmentation chain transfer radical polymerization (RAFT) mediated by benzyl dithioisobutyrate. The comonomer feeding rate profiles for the targeted distributions were designed from a newly developed computer model that was trained from the batch RAFT copolymerizations of St and BA at different monomer compositions. The semibatch copolymerization yielded precise copolymer products having their composition distributions exactly as targeted and the polymerization rate and molecular weight profiles as predicted by the model.

Introduction

Controlled/living free-radical polymerization (CLRP) provides a very powerful tool that allows precise control over polymer chain structure.[1−3] Numerous investigations have demonstrated that CLRP, particularly atom transfer radical polymerization (ATRP),[4,5] nitroxide-mediated polymerization (NMP),[6] and reversible addition−fragmentation chain transfer polymerization (RAFT),[7] can be used to synthesize a large variety of polymers with predetermined molecular weight and narrow molecular weight distribution as well as well-defined block, star, and brush architectures. CLRP has a clear advantage over other living polymerization such as anionic and cationic polymerization in terms of versatility of monomer types and mildness of reaction conditions. CLRP can be applied to homo- and copolymerization of a much larger variety of monomers.

Copolymerization plays an important role in tuning materials properties of polymer products. Controlled/living free-radical copolymerization (CLRcoP) of various comonomer pairs has been reported.[8−12] However, few studies focused on the control of copolymer composition distribution along individual chains. In a batch process, the relative consumption rates of different comonomers are governed by their respective reactivity ratios and cause a composition drifting. Therefore the composition distribution along polymer chains as synthesized is solely determined by the reactivity ratios of two monomers.[13−16] In CLRcoP, a majority of polymer chains are initiated in a relatively short period of time at the beginning of polymerization, followed by gradual growth. The "living" feature of CLRP gives individual chains a time period of hours to grow and allows us to design and control chain structure by a semibatch approach. Matyjaszewski et al.[17] and Torkelson et al.[18] used a constant comonomer feeding rate to prepare gradient copolymers by atom transfer radical polymerization. The resulting copolymers are one of a kind with novel chain composition distributions, which can only be obtained through living polymerization processes. There are some theoretical and experimental evidence that the composition distribution along a copolymer chain can be a new parameter of chain microstructure for fine-tuning morphologies at a nanoscale and thus mechanical properties of polymer materials. Matyjaszewski et al.[19] illustrated that the composition distribution can play a significant influence on tensile properties of brush polymers. Torkelson et al.[18] revealed that gradient copolymers having a linear composition distribution can form nanostructures, leading to a very wide range of glass transition.

In conventional free radical copolymerization, the copolymer compositions are often controlled based on online measurement and feedback technologies such as GC, NIR, calorimetry, etc.[20−22] However, little has been reported in the literature on the control of copolymer composition distribution in CLRcoP. Therefore a general approach with high flexibility for various copolymer composition distributions still provides a great challenge.

In this contribution, we aim at developing a model-based semibatch monomer feeding policy to tailor-make copolymer chain structure via CLRP. The RAFT copolymerization of styrene (St)/butyl acrylate (BA) is chosen as a working example. A kinetic model that takes into account diffusion-controlled termination is combined with a stirred tank reactor model. The ability of this mathematic model to describe RAFT copolymerization is demonstrated by its application to the copolymerization of St/BA.

Theory

Kinetic Model for Batch RAFT Copolymerization. A general kinetic model for the batch RAFT copolymerization is derived as shown in the Appendix. The model is based on the elementary reactions summarized in Table 1. An implicit penultimate model is used, i.e., both terminal and penultimate

* Corresponding authors. E-mail: yingwu.luo@zjuem.zju.edu.cn (Y.L.); bgli@zju.edu.cn (B-G.L.); zhuship@mcmaster.ca (S.Z.).
[†] Zhejiang University.
[‡] Zhejiang University of Science and Technology.
[§] McMaster University.

10.1021/ma061677v CCC: $37.00
Published on Web 01/26/2007

Table 1. Elementary Reactions Involved in Raft Copolymerization[25]

reaction type	scheme
initiation	$I \xrightarrow{f,k_d} 2P_0^\bullet$
	$P_0^\bullet + M_j \xrightarrow{k_{i,j}} P_{1,j}^\bullet$
propagation	$P_{r,ij}^\bullet + M_k \xrightarrow{k_{p,ijk}} P_{r+1,jk}^\bullet, \quad r = 1, 2, ...$
pre-equilibrium	$P_{r,ij}^\bullet + TP_0 \xleftrightarrow{k_{a,j}/k_{f,j}} P_{r,ij}\dot{T}P_0 \xleftrightarrow{k_{a,0}/k_{f,0}} P_0^\bullet + TP_{r,ij}$
core-equilibrium	$P_{r,ij}^\bullet + TP_{s,kl} \xleftrightarrow{k_{a,j}/k_{f,j}} P_{r,ij}\dot{T}P_{s,kl} \xleftrightarrow{k_{a,l}/k_{f,l}} P_{s,kl}^\bullet + TP_{r,ij}$
termination	$P_{r,ij}^\bullet + P_{s,kl}^\bullet \xrightarrow{k_{tc,jl}} P_{s+r}$
	$P_{r,ij}^\bullet + P_{s,kl}^\bullet \xrightarrow{k_{td,jl}} P_r + P_s$
	$P_{r,ij}^\bullet + P_{s,kl}\dot{T}P_{t,mn} \xrightarrow{k_{ct}} P_{r+s+t}$

Table 2. Definition of Various Chain Moments and Relationships between Intermediate Radical Chain Moments

type of chains	definition of moments
propagating radical	$Y_m^{ij} = \sum_{r=2}^{\infty} r^m [P_{r,ij}^\bullet]$
dormant	$Z_m^{ij} = \sum_{r=2}^{\infty} r^m [TP_{r,ij}]$
primary intermediate radical	$T_m^{ij} = \sum_{r=2}^{\infty} r^m [P_{r,ij}\dot{T}P_0]$
intermediate radical	$X_m^{ij,kl} = \frac{1}{2}\sum_{r=2}^{\infty} r^m \sum_{s=2}^{r-2} [P_{s,ij}\dot{T}P_{r-s,kl}] \quad (i = k, j = l)^a$
	$X_m^{ij,kl} = \sum_{r=2}^{\infty} r^m \sum_{s=2}^{r-2} [P_{s,ij}\dot{T}P_{r-s,kl}] \quad (i \neq k) \text{ or } (j \neq l)^a$
	$X_{m,n}^{ij,kl} = \sum_{r=2}^{\infty}\sum_{s=2}^{\infty} r^m s^n [P_{r,ij}\dot{T}P_{s,kl}]^b$
dead	$Q_m = \sum_{r=2}^{\infty} r^m [P_r]$
relationships between $X_m^{ij,kl}$ and $X_{m,n}^{ij,kl}$	For $i = k, j = l$: $X_0^{ij,kl} = {}^1/_2 X_{0,0}^{ij,kl}$, $X_1^{ij,kl} = X_{1,0}^{ij,kl}$, $X_2^{ij,kl} = X_{2,0}^{ij,kl} + X_{1,1}^{ij,kl}$ For $i \neq k$ or $j \neq l$: $X_0^{ij,kl} = X_{0,0}^{ij,kl}$, $X_1^{ij,kl} = X_{1,0}^{ij,kl} + X_{0,1}^{ij,kl}$, $X_2^{ij,kl} = X_{2,0}^{ij,kl} + 2X_{1,1}^{ij,kl} + X_{0,2}^{ij,kl}$

[a] The counting of intermediate radical chains with identical terminal/penultimate moieties and different chain lengths are different, the factor $^1/_2$ accounts for the fact that the summation s from 2 to r-2 double-counts such chain species. The intermediate chains of different terminal/penultimate moieties do not have this problem. [b] The definition of this moment is necessary for the closure of the differential moment equations.

units of a polymer radical affect its reactivity, but only the terminal unit affects its selectivity.[23] The implicit penultimate model has been proven to be sufficient for describing the conventional St/BA copolymerization kinetics.[24]

As listed in Table 2, five types of chain species are involved in the reaction system, i.e., propagating radical chains ($P_{r,ij}^\bullet$), dormant chains ($TP_{r,ij}$), primary intermediate radical chains ($P_{r,ij}\dot{T}P_0$), intermediate radical chains ($P_{r,ij}\dot{T}P_{s,kl}$), and dead chains (P_r). The notations $P_{r,ij}^\bullet$, $TP_{r,ij}$, and $P_{r,ij}^\bullet TP_0$ stand for propagating radical, dormant chain, and primary intermediate radical chains with chain length r,i-type penultimate unit, and j-type terminal unit; $P_{r,ij}^\bullet TP_{s,kl}$ stands for intermediate radicals that have two "arms" with chain lengths r and s, adjacent penultimate units i and k, and adjacent terminal units j and l, respectively. The kinetic equations for each type of chains in a batch reactor are summarized in Table 6. As in our previous work,[26] the method of moments is also used in this model development. The moment of chain species is defined in Table 2.

With the defined moments, the number-average chain length, weight-average chain length, polydispersity, and molar fractions of living polymer chains can be calculated accordingly,

$$\bar{r}_N = \frac{\sum_i\sum_j\sum_k\sum_l (Y_1^{ij} + Z_1^{ij} + T_1^{ij} + X_1^{ij,kl} + Q_1)}{\sum_i\sum_j\sum_k\sum_l (Y_0^{ij} + Z_0^{ij} + T_0^{ij} + X_0^{ij,kl} + Q_0)} \quad (1)$$

$$\bar{r}_W = \frac{\sum_i\sum_j\sum_k\sum_l (Y_2^{ij} + Z_2^{ij} + T_2^{ij} + X_2^{ij,kl} + Q_2)}{\sum_i\sum_j\sum_k\sum_l (Y_1^{ij} + Z_1^{ij} + T_1^{ij} + X_1^{ij,kl} + Q_1)} \quad (2)$$

$$\text{PDI} = \frac{\bar{r}_W}{\bar{r}_N} \quad (3)$$

$$N_{\text{living}} = \frac{\sum_i\sum_j Z_0^{ij}}{\sum_i\sum_j\sum_k\sum_l (Y_0^{ij} + Z_0^{ij} + T_0^{ij} + X_0^{ij,kl} + Q_0)} \quad (4)$$

After some mathematical manipulations, a complete set of moment equations combined with the mass balance equations of all the species in the reaction system can be obtained, as

attached in Table 7. Since the current work focuses on copolymerization rate and copolymer composition, we neglect the dependence of addition, fragmentation, and termination rate coefficients on chain length and penultimate unit type.

Diffusion-Controlled Termination Model. In free-radical polymerization, when the polymerization proceeds to intermediate and high conversions, the system becomes viscous and the reactants experience diffusion limitations. In this work, we consider diffusion-controlled termination reactions. On the basis of an encounter-pair model, the relative contributions of chemical activation and diffusion to the termination rate constant can be expressed as follows,[27−29]

$$\frac{1}{k_{tii}} = \frac{1}{k_{tii,C}} + \frac{1}{k_{tii,D}} \qquad (i = 1,2) \tag{5}$$

which can be applied to both disproportionation and recombination termination. Equation 5 describes the relative contributions of the chemically and diffusion-controlled termination reactions and provides a smooth transition from one to the other during polymerization.

The diffusion-controlled rate coefficients can be calculated using the following free-volume-based semiempirical expressions,[30]

$$k_{tii,D} = k_{tii,D}{}^{0}(\bar{r}_N)^{-2} \exp(-1/\nu_f) \tag{6}$$

where $k^0_{tii,D}$ is an adjustable parameter to correlate the experimental data. The free volume fraction ν_f is related to polymer concentration by[31,32]

$$\nu_f = [0.025 + \alpha_p(T - T_{gp})]\varphi_p + [0.025 + \alpha_{m1}(T - T_{gm1})]\varphi_{m1} + [0.025 + \alpha_{m2}(T - T_{gm2})]\varphi_{m2} + [0.025 + \alpha_s(T - T_{gs})]\varphi_s \tag{7}$$

where α is the thermal expansion coefficients, φ is the volume fractions, and T_g is the glass-transition temperatures. The subscripts p, m_i, and s denote polymer, monomer, and solvent, respectively. T_{gp} can be calculated from the Barton equation.[33]

Semibatch Reactor Model. The objective of this work is to design and control the composition distribution along copolymer chains through semibatch operations. We need to develop a reactor model for the semibatch polymerization. In this work, a well-mixed isothermal tank reactor is assumed. Because initiator and RAFT agent are in trace amounts, only monomer, solvent, and polymer significantly contribute to volume V and density ρ. In a semibatch reactor, applying mass balance for all entities yields

$$\frac{d(V\rho)}{dt} = V_f\rho_f \tag{8}$$

$$\text{i.e. } \frac{dV}{dt} = \frac{V_f\rho_f}{\rho} - \frac{V}{\rho}\frac{d\rho}{dt} \tag{9}$$

where V_f is the volumetric feeding rate and ρ_f is the density of feeding materials. The mass balance equations for species i are

$$\frac{d(VC_i)}{dt} = V_fC_{i,f} + VR_i \tag{10}$$

$$\text{i.e., } \frac{dC_i}{dt} = \frac{1}{V}\left(V_fC_{i,f} - C_i\frac{dV}{dt}\right) + R_i \tag{11}$$

where $C_{i,f}$ and C_i are the concentrations of species i in feed and in reactor; R_i is the reaction rate of species i, as expressed in Table 7.

The reaction volume is formulated as:

$$\frac{dV}{dt} = V_{s,in} + \sum_{i=1}^{2} F_{i,in}mw_{mi}/\rho_{mi} - \sum_{i=1}^{2} R_{p,i}mw_{mi}\left(\frac{1}{\rho_{mi}} - \frac{1}{\rho_p}\right)V \tag{12}$$

where $V_{s,in}$ is the volumetric flow rate of solvent into the reactor, $F_{i,in}$ is the molar flow rate of monomer i into the reactor, mw_{mi} is the molecular weight of i-type monomer, and ρ is the density.

Programmed Synthesis. The reactor model (eqs 10, 11, and 12), together with the mass balance equations of various species in Table 7, form a complete set of equations for the semibatch RAFT copolymerization. When the initial conditions are given, the equations can be solved simultaneously with a commercial ordinary differential equation (ODE) solver (ode15s in MATLAB 7.1). By solving the ODEs, the monomer concentration, degree of polymerization, and distribution can be calculated at any given time. The rate of polymerization and copolymer composition can then be calculated from,

$$\text{Monomer conversion } (X): \ X = \frac{\sum_{i=1}^{2}(M_{i0} - M_{it} - M_{ir})}{\sum_{i=1}^{2} M_{i0}} \tag{13}$$

Cumulative copolymer composition (F_{ni}):

$$F_{ni} = \frac{M_{i0} - M_{it} - M_{ir}}{\sum_{j=1}^{2}(M_{j0} - M_{jt} - M_{jr})} \tag{14}$$

Number-average molecular weight (M_n):

$$M_n = \sum_{i=1}^{2} \bar{r}_N F_{ni} mw_{mi} \tag{15}$$

where M_{i0} is the total mole of monomer i. M_{it} and M_{ir} are the moles of monomer i in the tank and in the reactor, respectively. On the other hand, when a specific type of chain microstructure (i.e., the copolymer composition distribution in this work) is targeted, we can design the feeding rate versus time profile by solving the ODE's off line under the constraint equation that describes the chain microstructure. The feeding rate is controlled by a metering pump that is programmed with the designed profile.

Experimental

Materials. Styrene (Shanghai Ling Feng Chemical Reagent Co., 99%) and BA (Shanghai Chemical Reagent Co., 98%) were purified by vacuum distillation. 2,2′-Azobis(isobutyronitrile) (AIBN, Shanghai Si He Chemical Reagent Co., LTD, 98%) was purified by recrystallization from methanol. Benzyl dithioisobutyrate (BDIB) was synthesized according to the procedure reported in the Supporting Information. All other chemicals were commercially obtained and used without purification.

Polymerization Recipes. The bulk RAFT homopolymerizations of St (run 1a) and BA (run 1b) were performed first to investigate the mediation abilities of BDIB. To systematically examine the influence of BDIB and monomer composition on the polymerization kinetics, the experiments were designed as follows. Runs 2a−2b and runs 3a−3d were used to investigate the influence of BDIB

Table 3. Recipes Used for the Experimental Runs of St/BA Raft Polymerization[a]

expt	St (g)	BA (g)	initial St molar fraction, $f_{St,0}$	total St molar fraction	toluene (g)	$[AIBN]_0$ (mmol/l)	$[RAFT]_0$ (mmol/l)	DPn
1a	35		1			8.4	25.20	333
1b		35	0			9.2	27.60	333
2a	15		1		15	7		
2b	15		1		15	7	20.82	200
3a		11	0		11	7		
3b		11	0		11	7	10.03	333
3c		11	0		11	7	20.06	167
3d		11	0		11	7	16.72	200
4c	3.12	11.52	0.25		14.65	7	17.60	200
5c	6.25	7.68	0.5		13.93	7	18.60	200
6c	9.38	3.84	0.75		13.22	7	19.62	200
7d	5.94[b]	76.80[b]	0.087[b]	0.25	82.74[b]	8.2[b]	20.72[b]	200
8d	0[b]	76.80[b]	0[b]	0.25	76.80[b]	5.6[b]	22.30[b]	200

[a] St: styrene; BA: butyl acrylate; AIBN: 2,2′-azobis(isobutyronitrile); RAFT: benzyl dithioisobutyrate (BDIB); DPn: degree of polymerization or number-average chain length [b] The recipe for the first stage in expts 7d and 8d.

Scheme 1. Schematic Experimental Setup for the Semibatch RAFT Polymerization

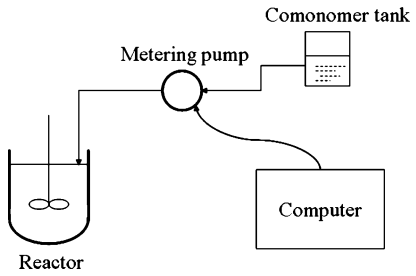

on the St and BA solution RAFT homopolymerizations, while runs 2b, 3d, 4c, 5c, and 6c were designed to study the monomer composition effects. Finally, runs 7d and 8d targeted for the copolymers with uniform and linear gradient composition, respectively. All the polymerization recipes are summarized in Table 3.

Batch Copolymerization. The mixture of St, BA, toluene (only for the solution polymerization), AIBN, and BDIB was transferred to individual ampoules, followed by deoxygenation with purified nitrogen for five times. The ampoules sealed with septa were bathed in 70 °C water, and each ampule was removed at a preset time. The reaction was quenched by cooling the solution in an ice bath, and a small amount of hydroquinone was added to stop the polymerization. The polymer materials were collected by evaporating the solvent and residual monomer. The final conversions were measured by gravimetry.

Semibatch Solution Copolymerization. A solution of St, BA, toluene, and BDIB was initially charged to a 500 mL five-neck flask, equipped with a condenser, a nitrogen inlet, a mechanical stirrer, and a syringe pump. Scheme 1 shows the experimental setup. The solution was stirred at room temperature for 20 min before immersed into a water bath at 70 °C. The reactor, deoxygenated for 30 min before the solution was charged, was further deoxygenated by purging it with nitrogen for 10 min. The polymerization was started by adding AIBN that was dissolved in 5 g toluene. The deoxygenized comonomer was continuously fed to the reactor according to a programmed feeding rate controlled by a computer. The samples were regularly withdrawn and quenched with hydroquinone.

^{1}H NMR. ^{1}H NMR spectroscopy (Avance DMX500 spectrometer operated at 500 MHz) was used to determine the copolymer composition. Spectra were recorded at room temperature. The polymer solutions were about 8% (w/v) in deuterated chloroform. The relative amounts of comonomers incorporated in polymer chains were estimated from the areas under designated peaks. For St/BA copolymers, the peaks at approximately 6.5 ppm were assigned to the five protons on the benzene ring of St, while the peaks at approximately 3.5 ppm were assigned to the two protons of the methylene group close to the oxygen in the ester moiety of BA. The copolymer composition was determined from the integrated intensities of these resonance signals.

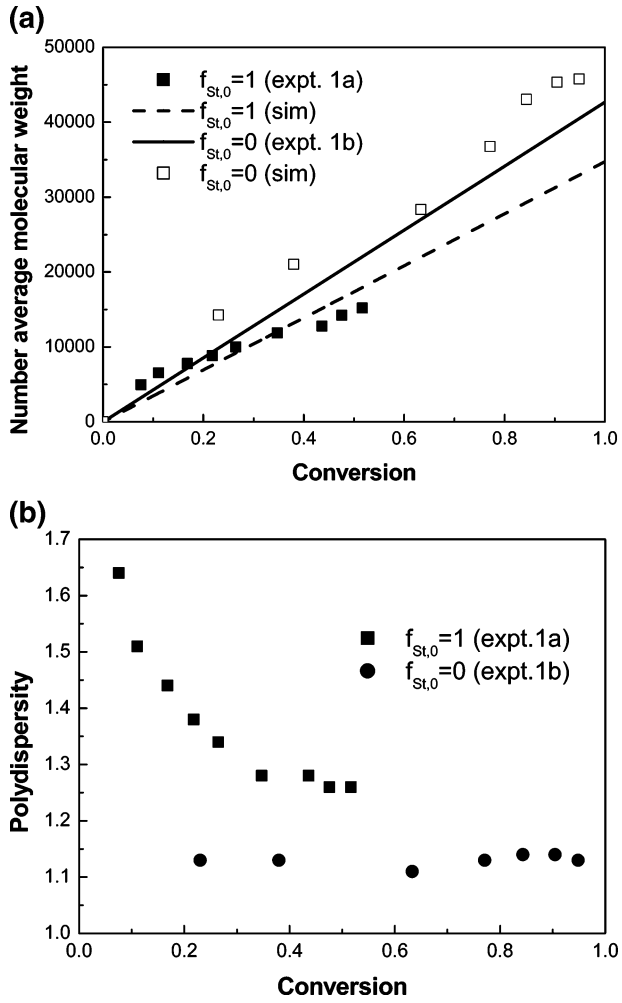

Figure 1. (a) Molecular weight vs conversion and (b) polydispersity index vs conversion for the bulk St and BA homopolymerizations in batch at 70 °C with AIBN as initiator and BDIB as RAFT agent (run 1a: $[St]_0/[BDIB]_0/[AIBN]_0 = 1000:3:1$; run 1b: $[BA]_0/[BDIB]_0/[AIBN]_0 = 1000:3:1$).

GPC. Molecular weight and molecular weight distribution of the copolymers were determined at 30 °C by GPC (Waters 2487/630C) with three PL columns (10000, 1000, and 500 Å). The eluent was THF, with a flow rate of 1 mL/min. The measurement was calibrated using narrow PS standard samples with molecular weight ranging from 580 to 710 000 g/mol.

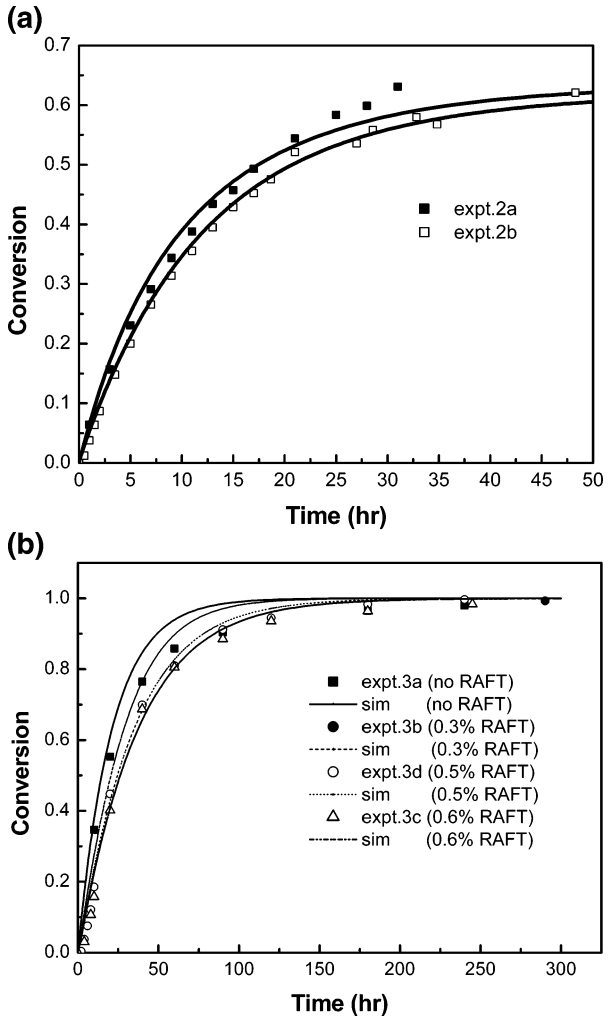

Figure 2. (a) Monomer conversion vs time of the batch polymerization of styrene mediated by BDIB in toluene at 70 °C. AIBN: 7 mmol/L; BDIB (run 2a: 0; run 2b: 20.82 mmol/L). (b) Monomer conversion vs time of the batch polymerization of butyl acrylate mediated by BDIB in toluene at 70 °C. AIBN: 7 mmol/L; BDIB (run 3a: 0; run 3b: 10.03 mmol/L; run 3c: 20.06 mmol/L; run 3d: 16.72 mmol/L). The curves are the simulation results. For the RAFT-free systems, $k^0_{t11,D} = 2.3 \times 10^{16}$ and $k^0_{t22,D} = 1 \times 10^{20}$ are used.

Results and Discussion

1. Homopolymerization of St and BA Mediated by BDIB. The mediation abilities of the RAFT agent BDIB in St and BA homopolymerizations and their polymerization kinetics were first investigated. The results are presented in Figures 1 and 2. Figure 1a shows that, in both systems, M_n increased linearly with monomer conversion. At low conversions, the M_n data in St polymerization were higher than the theoretical values (calculated from the concentration ratio of converted monomer over initially charged RAFT agent), suggesting that some of the BDIB molecules were not converted into polymer chains at the low conversions. The M_n data of BA polymerization were also higher than the theoretical values during the whole course of polymerization, which can be ascribed to differences in the hydrodynamic volumes of PBA and PSt (as the calibration standard). The polydispersity indexes of the polymer samples were low, as seen in Figure 1b. It can be concluded that the polymerizations proceeded in a controlled manner. BDIB worked better for BA than for St, as indicated by the lower PDI's of the former polymer. In the case of St, the PDI was high at the beginning but decreased to a level of 1.25.

Table 4. Values of Addition and Fragmentation Rate Coefficients Used in the Simulation for St/BA Raft Polymerization

$k_{a,0}$ $(M^{-1}\,s^{-1})$[37]	$k_{a,1}$ $(M^{-1}\,s^{-1})$[37]	$k_{a,2}$ $(M^{-1}\,s^{-1})$[37]	$k_{f,0}$ (s^{-1})[41]	$k_{f,1}$ (s^{-1})[41]	$k_{f,2}$ (s^{-1})[36]
4×10^6	4×10^6	4×10^6	4×10^5	4×10^5	80

Table 5. Model Parameters Estimated from Data Correlation in St/BA Raft Polymerization

$\langle k_{ct}\rangle/\langle k_t\rangle$[a]	$k^0_{t11,D}$	$k^0_{t22,D}$
$0.001\exp(-f_{St}/0.02)$	1.5×10^{14}	1×10^{15}

[a] $\langle k_t\rangle = p_1^2 k_{t,11} + 2p_1p_2k_{t,12} + p_2^2k_{t,22}$, where p_i is the relative concentration of the terminal radical i.

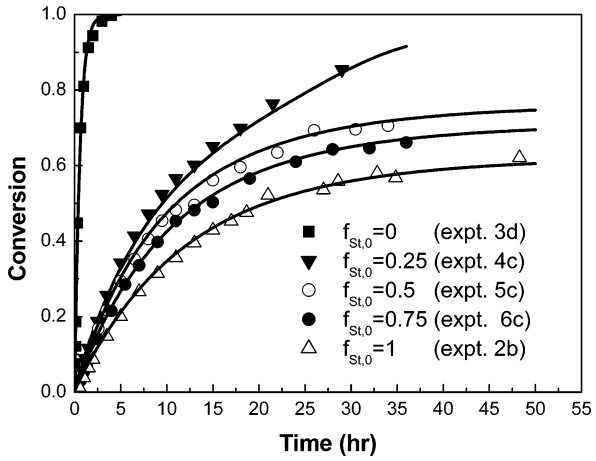

Figure 3. Comparison of model prediction and experimental data of the monomer conversion of St and BA with five different initial monomer ratios. Temperature 70 °C; AIBN: 7 mmol/L; $[monomer]_0/[BDIB]_0 = 200{:}1$; solid content: 50%; initial/monomer ratio: run 3d: $f_{St,0} = 0$; run 4c: $f_{St,0} = 0.25$; run 5c: $f_{St,0} = 0.5$; run 6c: $f_{St,0} = 0.75$; run 2b: $f_{St,0} = 1$.

Figure 2a shows the evolution of monomer conversion with time for the St/BDIB system with and without BDIB addition (i.e., $c^0_{BDIB} = 0$ and $c^0_{BDIB} = 20.82$ mmol/L) at 70 °C (runs 2a and 2b). The limited conversion was due to its low propagation rate constant and depletion of the initiator amount. The polymerization rate for the RAFT system was almost the same as that for the RAFT-free system at low conversions. In this regard, there was little effect of RAFT process on the polymerization rate.[34] However, the polymerization rate of the RAFT-free system became higher at the late stage of polymerization. This is probably because the RAFT polymerization has a weaker gel effect than its RAFT-free counterpart.[35] Figure 2b shows the conversion versus time for the polymerization of BA in the presence of BDIB at 70 °C (runs 3a−3d). The curves exhibited an S-shape at low conversions in the presence of RAFT agent, suggesting the existence of an induction period. The polymerization rate decreased with increased BDIB concentration. This result can be explained by a higher apparent equilibrium constant for the BA/BDIB system than for the St/BDIB system.[36]

2. Batch Copolymerization of St and BA and Model Correlation. Our primary motivation for this work is to develop a general method through a model-based computer-controlled semibatch comonomer feeding policy to tailor copolymer chain structure in CLRP. Thus, a kinetic model with a set of appropriate parameters needs to be developed. The kinetic rate constants for the RAFT-free St (monomer 1)/BA (monomer 2) copolymerization are obtained from the literature and summarized in Table 8. The physical and transport parameters for the diffusion-controlled termination reaction are listed in Table 9.

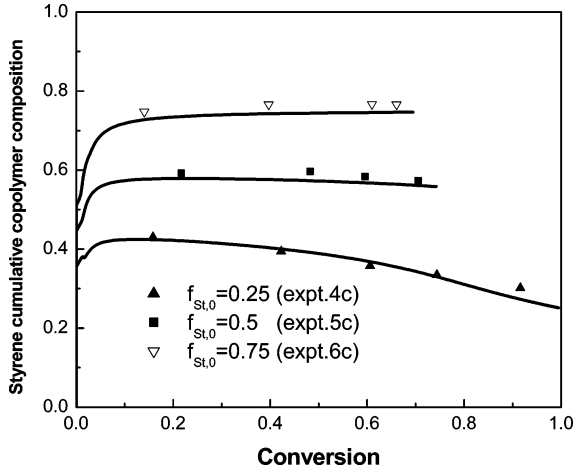

Figure 4. Comparison of model prediction and experimental data for the cumulative styrene copolymer composition vs total monomer conversion of the St/BA RAFT copolymerization with three different initial monomer ratios. The experiment conditions are the same as in Figure 3.

Because there were few kinetic data related to the polymerization mediated by BDIB in the literature, we used the addition and fragmentation rate coefficients of a RAFT agent with similar structure, as in Table 4. There is an ongoing debate about the order of magnitude of the fragmentation rate coefficients, particularly for styrene/4-cyanopentanoic acid dithiobenzoate (CPDB) system. The rate retardation observed in the RAFT polymerization was ascribed to either cross-termination between propagating and intermediate radicals with fast fragmentation rate[37,38] or to radical sinking derived from slow fragmentation rate.[39] Both mechanisms can provide adequate explanation to the phenomenon of rate retardation. Recently, the existence of the cross-termination has been established. However, the magnitude of the fragmentation rate coefficient remains ambiguous.[40] The cross-termination is included in the present model. This mechanism is supported by our direct measurement of the fragmentation rate coefficient via RAFT miniemulsion polymerization.[41] Because the *Z* group of the RAFT agent used in the present work is an isopropyl moiety, it is believed that the *Z* group is weaker in stabilizing the intermediate radicals than phenyl but close to that of benzyl. The fragmentation rate coefficient of styrene/1-phenylethyl phenyldithioacetate (PEPDTA) is estimated to be 2×10^5 s^{-1}. The fragmentation rate coefficient of St of the current system is set to be 4×10^5 s^{-1}, which is in good accordance with the small rate retardation of the styrene polymerization mediated by the current RAFT agent, as seen in Figure 2a. As shown in Figure 2b, there is significant retardation in the BA polymerization rate mediated by the current RAFT agent. The fragmentation rate coefficient in the BA polymerization is expected to be much lower than that of St polymerization and set to 80 s^{-1}. Actually, the exact value is not critical to predict the polymerization rate. The intrinsic RAFT polymerization rate can be related to the RAFT-free system by[37]

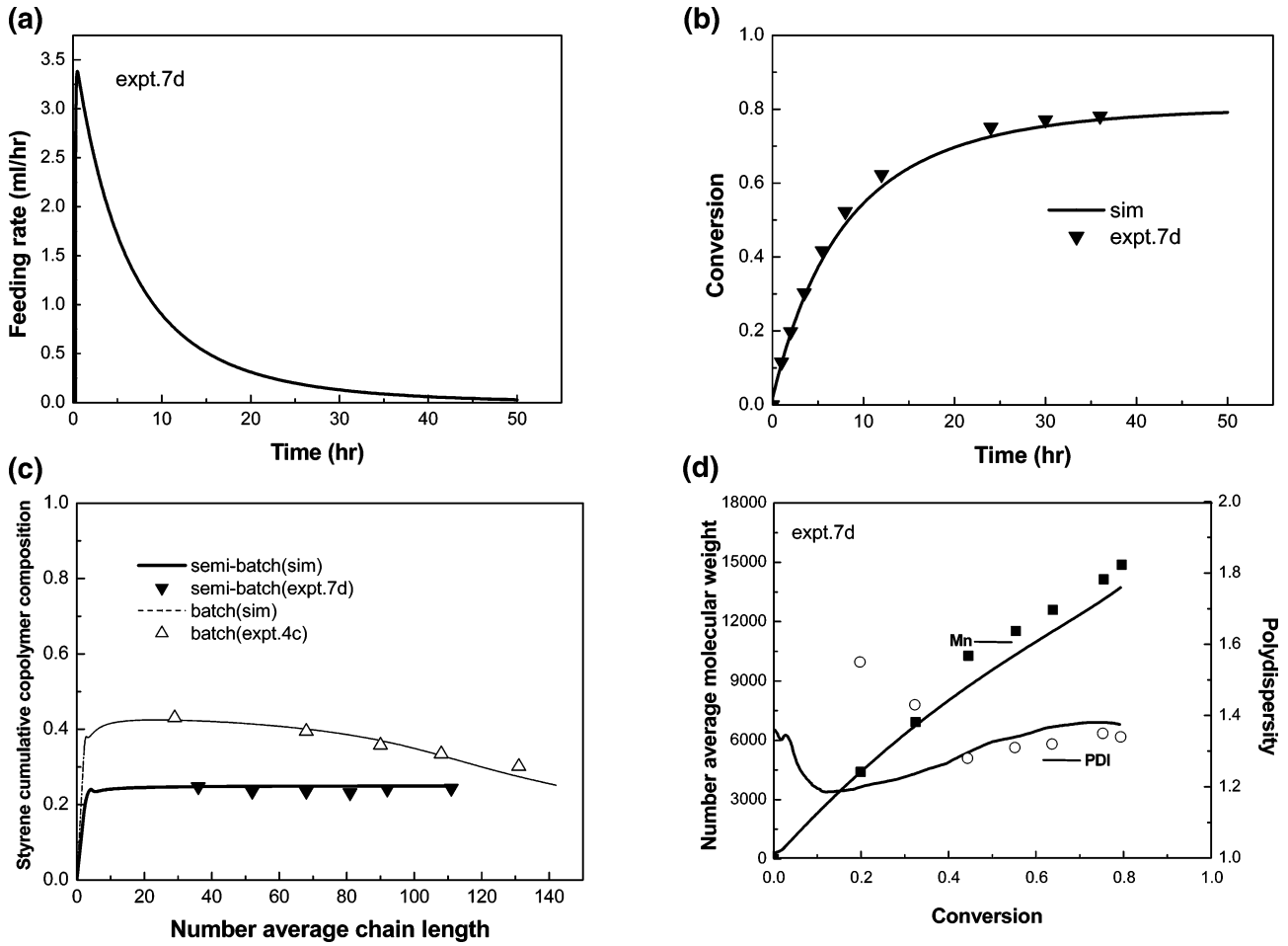

Figure 5. (a) Programmed volumetric feeding rate vs time profile, (b) polymerization rate vs time, (c) cumulative styrene copolymer composition vs number average chain length, (d) number-average molecular weight and polydispersity vs conversion of the semibatch St/BA RAFT copolymerzation that targets for the uniform composition distribution of $F_1 = 0.25$ (run 7d). The points are experimental data, while the lines are theoretical predictions. Also shown in (c) is the corresponding batch copolymerization result for comparison (run 4c).

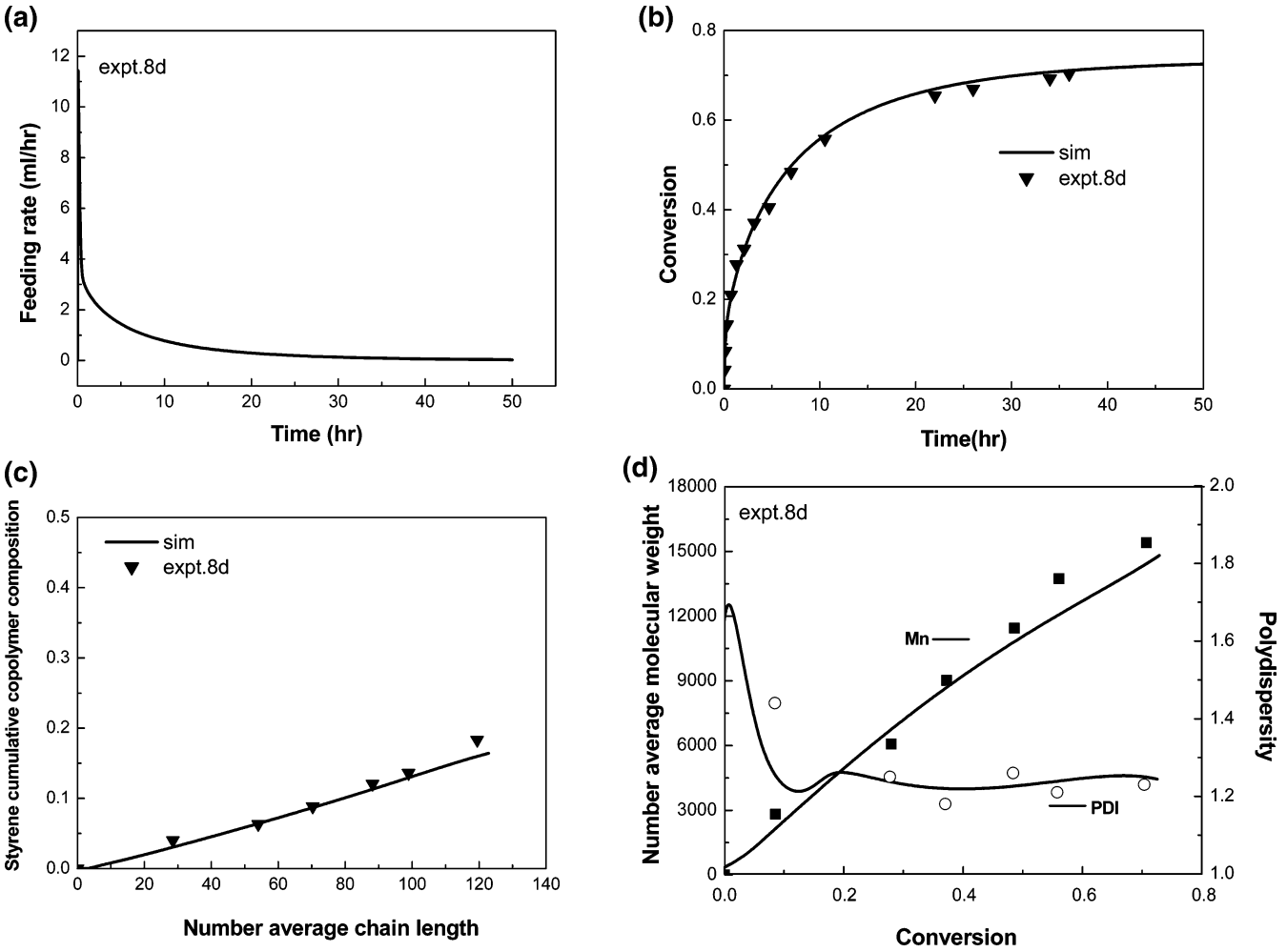

Figure 6. (a) Programmed volumetric feeding rate vs time, (b) polymerization rate vs time, (c) cumulative styrene copolymer composition vs number-average chain length, (d) number-average molecular weight and polydispersity vs conversion of the semibatch St/BA RAFT copolymerization that targets for the linear gradient copolymer $F_1 = 0.5 \times \bar{r}_N/\bar{r}_{N,\text{targeted}}$ (run 8d).

$$R_P^{-2} = R_{P,0}^{-2}\{1 + 2(k_{ct}/k_t)K[\text{RAFT}]_0\}$$

It is seen that the extent of retardation is determined by the product of two group parameters K and k_{ct}/k_t. It is difficult to separate their individual effect from the rate data. In the current study, the apparent RAFT equilibrium constant is fixed because the addition and fragmentation rate coefficients are preset. The value of $\langle k_{ct}\rangle/\langle k_t\rangle$ at five initial St mole fractions ($f_{St,0} = 0$, 0.25, 0.5, 0.75, 1) are optimized respectively by fitting the kinetics data at low conversions with the least-square fitting method. The function of $\langle k_{ct}\rangle/\langle k_t\rangle$ against comonomer composition can then be obtained, as shown in Table 5. The adjustable parameter for the diffusion-controlled termination, $k^0_{tii,D}$, is determined by fitting the experimental data at high conversions.

Figure 3 compares the calculation (lines) to the experimental data (points). The polymerization rate decreased as the initial St mole fraction ($f_{St,0}$) increased due to the lower value of styrene propagation rate constant. The agreements are very good. Figure 4 shows the dependence of styrene-cumulative copolymer composition on the total molar monomer conversion. The model prediction agreed well with the experimental data for the three different $f_{St,0}$ values. It becomes clear that the model is predictive not only for the polymerization rate but also for the copolymer composition.

3. Programmed Synthesis of Copolymer with Uniform Composition. We designed a copolymer with uniform chain composition at $F_1 = 0.25$ and $M_n = 24\,400$ g/mol. To synthesize such a copolymer product, the full amount of BA was charged to the reactor at the very beginning of polymerization. The amount of St initially charged to the reactor was calculated from the Mayo−Lewis equation with the targeted copolymer composition ($F_1 = 0.25$) (run 7d). Shortly after the copolymerization

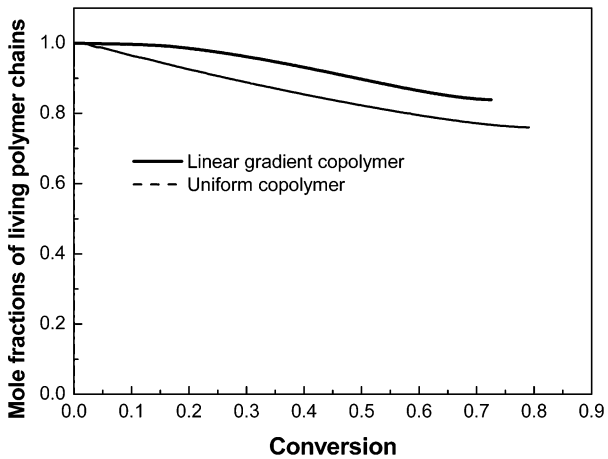

Figure 7. The molar fractions of living polymer chains vs number-average chain length of the semibatch St/BA RAFT copolymerization that targets for a uniform composition distribution of $F_1 = 0.25$ and the linear gradient copolymer $F_1 = 0.5 \times \bar{r}_N/\bar{r}_{N,\text{targeted}}$

Table 6. Kinetic Equations for Each Chain Species Involved in St/BA RAFT Copolymerization

type of chain	mass balance equation
propagating radical chain	$\frac{d[P^{\bullet}_{r,ij}]}{dt} = \sum_k k_{p,kij}[P^{\bullet}_{r-1,ki}][M_j] - \sum_k k_{p,ijk}[P^{\bullet}_{r,ij}][M_k] - k_{a,j}[P^{\bullet}_{r,ij}]([TP_0] + \sum_k \sum_l \sum_s [TP_{s,kl}]) + \frac{1}{2} k_{fj}\left([P_{r,ij}\dot{T}P_0] + \frac{1}{2}\sum_k \sum_l \sum_s [P_{r,ij}\dot{T}P_{s,kl}]\right) - \sum_k \sum_l \sum_s (k_{tc,jl} + k_{td,jl})[P^{\bullet}_{r,ij}][P^{\bullet}_{s,kl}] - k_{ct}[P^{\bullet}_{r,ij}](\sum_k \sum_l \sum_s [P_{s,kl}\dot{T}P_0] - \sum_k \sum_l \sum_m \sum_n \sum_s \sum_t [P_{s,kl}\dot{T}P_{t,mn}])$
dormant chain	$\frac{d[TP_{r,ij}]}{dt} = \frac{1}{2}\left(k_{f,0}[P_{r,ij}\dot{T}P_0] + \frac{1}{2}\sum_k \sum_l \sum_s k_{f,l}[P_{r,ij}\dot{T}P_{s,kl}]\right) - (k_{a,0}[P^{\bullet}_0] + \sum_k \sum_l \sum_s k_{a,l}[P^{\bullet}_{s,kl}])[TP_{r,ij}]$
primary intermediate radical chain	$\frac{d[P_{r,ij}\dot{T}P_0]}{dt} = k_{a,0}[P^{\bullet}_0][TP_{r,ij}] + k_{a,j}[P^{\bullet}_{r,i,j}][TP_0] - \frac{1}{2}(k_{f,0} + k_{fj})[P_{r,i,j}\dot{T}P_0] - \sum_k \sum_l \sum_s k_{ct}[P^{\bullet}_{s,kl}][P_{r,ij}\dot{T}P_0]$
intermediate radical chain	$\frac{d[P_{r,ij}\dot{T}P_{s,kl}]}{dt} = k_{a,j}[P^{\bullet}_{r,ij}][TP_{s,kl}] + k_{a,l}[P^{\bullet}_{s,k,l}][TP_{r,i,j}] - \frac{1}{2}(k_{fj} + k_{f,l})[P_{r,ij}\dot{T}P_{s,kl}] - \sum_m \sum_n \sum_t k_{ct}[P^{\bullet}_{t,mn}][P_{r,ij}\dot{T}P_{s,kl}]$
dead chain	$\frac{d[P_r]}{dt} = \sum_i \sum_j \sum_k \sum_l \sum_{s=0}^{r} k_{tc,jl}[P^{\bullet}_{s,ij}][P^{\bullet}_{r-s,kl}] + \sum_i \sum_j \sum_k \sum_l \sum_s k_{td,jl}[P^{\bullet}_{r,ij}][P^{\bullet}_{s,kl}] + \sum_i \sum_j \sum_k \sum_l \sum_{s=0}^{r} k_{ct}[P^{\bullet}_{s,ij}][P_{r-s,kl}\dot{T}P_0] + \sum_i \sum_j \sum_k \sum_l \sum_m \sum_n \sum_{s=0}^{r} k_{ct}[P^{\bullet}_{r-s,ij}] \sum_{t=0}^{s} [P_{t,kl}\dot{T}P_{s-t,mn}]$

started, the monomer concentration ratio of St over BA decreased because St was consumed more rapidly. The rest amount of St was charged to the reactor through a programmed metering pump. Incorporating the following constraint condition into the model, we obtained the volumetric feeding rate versus time profile as shown in Figure 5a through the model simulation

$$F_1 = \frac{R_{m1}}{R_{m1} + R_{m2}} = 0.25 \tag{16}$$

where R_{mi} is the consumption rate of monomer *i*.

Figure 5b shows the comparisons of the experimental data to the simulations for the molar conversion of St and BA versus time. The experimental data are in full agreement with the simulation. Figure 5c shows the copolymer composition distribution obtained with the programmed feeding profile. For comparison, the cumulative composition in a batch operation (i.e., the full amounts of both monomers are charged to the reactor at the beginning) are also shown in the figure. In the batch copolymerization, the composition clearly experienced drifting along the chain length. However, the copolymer product with the uniform distribution as designed was achieved through the programmed semibatch process. Figure 5d shows the development of the number-average molecular weight and polydispersity with respect to the total monomer molar conversion. The model successfully predicted the variation.

4. Programmed Synthesis of Copolymer with Linear Gradient Composition. Besides the uniform composition distribution, we also synthesized the copolymers with a targeted linear gradient composition distribution through the semibatch operation (run 8d). For $F_{n1} = 0.25$, the following constraint condition was applied

$$F_1 = \frac{0.5 \times \bar{r}_N}{\bar{r}_{N,\text{targeted}}} \tag{17}$$

Figure 6a shows the feeding profile calculated from the model. Figure 6b shows the resulting copolymer composition distribution along chain length. Figure 6c shows the rate of polymerization, and Figure 6d shows the development of molecular weight and polydispersity. In parts b, c, and d of Figure 6, the continuous lines represent the model prediction, while the discrete points denote the experimental data. Good agreements between the model prediction and experimental results were also obtained.

Another important property is the fraction of living polymer chains. This information is also provided in our simulation. The molar fractions of living polymer chains N_{living} are shown in Figure 7. It can be seen that, during the semibatch copolymerization process, the livingness of all chains in both uniform and linear gradient cases maintained a high level. The final molar fractions of living chains were around 80%.

Conclusion

In this work, we demonstrated the first use of semibatch RAFT copolymerization for the control over copolymer composition distribution of gradient copolymer. The approach was to feed comonomer to the reactor through a programmed metering pump. The feeding rate profile was designed based on a developed computer model. We applied this approach to the RAFT copolymerization of styrene (St) and butyl acrylate (BA) and targeted for the copolymer products having uniform and linear gradient composition distributions. The synthesized products had the exact composition distributions as targeted. The experimental polymerization rate and molecular weight profiles also agreed well with the model prediction.

We believe that the developed semibatch approach opens a new route to the precise design and control of polymer chain microstructure and thus materials properties. This approach is general and can be used for any targeted copolymer composition distributions. It is also applicable to other types of controlled/living radical polymerization such as ATRP and NMP.

Acknowledgment. We thank the National Science Foundation of China (NSFC) for award no. 20474057, no. 20204015, and a JB Award, the Ministry of Education of China for a Changjiang Scholar Visiting Fellowship as well as for New Century Excellent Talent in University, and Zhejiang University for supporting this research.

Supporting Information Available: Synthesis of benzyl dithioisobutyrate (BDIB), materials and procedure. This material is available free of charge via the Internet at http://pubs.acs.org.

Table 7. Differential Moment Equations

zeroth order moments) (i.e., molar conc of chains	propagating radical chains	$\frac{dY_0^{ij}}{dt} = k_{p,ij}[P^\bullet_{1,i}][M_j] + \sum_k k_{p,kij}[M_j]Y_0^{ki} - \sum_k k_{p,ijk}[M_k]Y_0^{ij} - k_{a,j}Y_0^{ij}([TP_0] + \sum_k \sum_l Z_0^{kl}) + \frac{1}{2}k_{f,j}(T_0^{ij} + \sum_{k\neq i}\sum_{orl\neq l} X_0^{ij,kl} + 2\sum_{k=i}\sum_{l=j} X_0^{ij,kl}) - [k_{tc,0}[P_0^\bullet] + \sum_k \sum_l (k_{tc,jl} + k_{td,jl})Y_0^{kl}]Y_0^{ij} - k_{ct}Y_0^{ij}([P_0\dot{T}P_0] + \sum_k \sum_l T_0^{kl} + \sum_k \sum_l \sum_m \sum_n X_0^{kl,mn})$
	dormant chains	$\frac{dZ_0^{ij}}{dt} = \frac{1}{2}(k_{f,0}T_0^{ij0} + \sum_k k_{f,k}T_0^{ijk} + \sum_{k\neq i}\sum_{orl\neq j} k_{f,l}X_0^{ij,kl} + 2\sum_{k=i}\sum_{l=j} k_{f,l}X_0^{ij,kl}) - (k_{a,0}[P_0^\bullet] + \sum_k \sum_l k_{a,l}Y_0^{kl})Z_0^{ij}$
	primary intermediate radical chains	$\frac{dX_0^{ij,kl}}{dt} = k_{a,j}Y_0^{ij}Z_0^{kl} - k_{f,j}X_0^{ij,kl} - k_{ct}X_0^{ij,kl}([P_0^\bullet] + + \sum_m \sum_n Y_0^{mn})$ $(i = k, j = l)$
	intermediate radical chains	$\frac{dX_0^{ij,kl}}{dt} = k_{a,j}Y_0^{ij}Z_0^{kl} - k_{f,j}X_0^{ij,kl} - k_{ct}X_0^{ij,kl}([P_0^\bullet] + + \sum_m \sum_n Y_0^{mn})$ $(i = k, j = l)$
		$\frac{dX_0^{ij,kl}}{dt} = k_{a,j}Y_0^{ij}Z_0^{kl} + k_{a,l}Y_0^{kl}Z_0^{ij} - \frac{1}{2}(k_{f,j} + k_{f,l})X_0^{ij,kl} - k_{ct}X_0^{ij,kl}([P_0^\bullet] + \sum_m \sum_n Y_0^{mn})$ $(i \neq k)$ or $(j \neq l)$
	dead chains	$\frac{dQ_0}{dt} = (k_{tc,0} + k_{td,0})[P_0^\bullet]\sum_i \sum_j Y_0^{ij} + \frac{1}{2}\sum_i \sum_j \sum_{k=i} \sum_{l=j} k_{tc,jl}Y_0^{ij}Y_0^{kl} + \sum_i \sum_j \sum_{k\neq i} \sum_{l\neq j} k_{tc,jl}Y_0^{ij}Y_0^{kl} + \sum_i \sum_j \sum_k \sum_l k_{td,jl}Y_0^{ij}Y_0^{kl} + k_{ct}[([P_0^\bullet] + \sum_i \sum_j Y_0^{ij})(\sum_i \sum_j T_0^{ij} + \sum_i \sum_j \sum_k \sum_l X_0^{ij,kl})]$
first-order moments (i.e., molar conc. of monomer units in chains)	propagating radical chains	$\frac{dY_1^{ij}}{dt} = 2k_{p,ij}[P^\bullet_{1,i}][M_j] + \sum_k k_{p,kij}[M_j]Y_0^{ki} + \sum_k k_{p,kij}[M_j]Y_1^{ki} - \sum_k k_{p,ijk}[M_k]Y_1^{ij} - 2\sum_{k=i=j} k_{p,ijk}[M_k]Y_0^{ij} - k_{a,j}Y_1^{ij}([TP_0] + \sum_k \sum_l Z_0^{kl}) + \frac{1}{2}k_{f,j}(T_1^{ij} + \sum_{k\neq i}\sum_{orl\neq l} X_{1,0}^{ij,kl} + \sum_{k=i}\sum_{l=j} X_1^{ij,kl}) - [k_{tc,ij}[P_0^\bullet] + \sum_k \sum_l (k_{tc,jl} + k_{td,jl})Y_0^{kl}]Y_1^{ij} - k_{ct}Y_1^{ij}([P_0\dot{T}P_0] + \sum_k \sum_l T_0^{kl} + \sum_k \sum_l \sum_m \sum_n X_0^{kl,mn})$
	dormant chains	$\frac{dZ_1^{ij}}{dt} = \frac{1}{2}(k_{f,0}T_1^{ij} + \sum_{k\neq i}\sum_{orl\neq j} k_{f,l}X_{1,0}^{ij,kl} + \sum_{k=i}\sum_{l=j} k_{f,l}X_1^{ij,kl}) - (k_{a,0}[P_0^\bullet] + \sum_k \sum_l k_{a,l}Y_0^{kl})Z_1^{ij}$
	primary intermediate radical chains	$\frac{dT_1^{ij}}{dt} = k_{a,0}[P_0^\bullet]Z_1^{ij} + k_{a,j}[TP_0]Y_1^{ij} - \frac{1}{2}(k_{f,0} + k_{f,j})T_1^{ij} - k_{ct}T_1^{ij}([P_0^\bullet] + \sum_k \sum_l Y_0^{kl})$
	intermediate radical chains	$\frac{dX_1^{ij,kl}}{dt} = k_{a,j}(Y_1^{ij}Z_0^{kl} + Y_0^{ij}Z_1^{kl}) - k_{f,j}X_1^{ij,kl} - k_{ct}X_1^{ij,kl}([P_0^\bullet] + \sum_m \sum_n Y_0^{mn})$ $(i = k, j = l)$
		$\frac{dX_1^{ij,kl}}{dt} = k_{a,j}(Y_1^{ij}Z_0^{kl} + Y_0^{ij}Z_1^{kl}) + k_{a,l}(Y_1^{kl}Z_0^{ij} + Y_0^{kl}Z_1^{ij}) - \frac{1}{2}(k_{f,j} + k_{f,l})X_1^{ij,kl} - k_{ct}X_1^{ij,kl}([P_0^\bullet] + \sum_m \sum_n Y_0^{mn})$ $(i \neq k)$ or $(j \neq l)$
		$\frac{dX_{1,0}^{ij,kl}}{dt} = k_{a,j}Y_1^{ij}Z_0^{kl} + k_{a,l}Y_0^{ij}Z_1^{kl} - \frac{1}{2}(k_{f,j} + k_{f,l})X_{1,0}^{ij,kl} - k_{ct}X_{1,0}^{ij,kl}([P_0^\bullet] + \sum_m \sum_n Y_0^{mn})^a$

Table 7 (Continued)

	dead chains	$\frac{dQ_1}{dt} = (k_{tc,0} + k_{td,0})[P_0^\bullet] \sum_i \sum_j Y_1^{ij} + \sum_i \sum_j \sum_k \sum_l (k_{tc,jl} + k_{td,jl}) Y_1^{ij} Y_0^{kl} + k_{ct}[([P_0^\bullet] + \sum_i \sum_j Y_0^{ij})(\sum_i \sum_j T_1^{ij} + \sum_i \sum_j \sum_k \sum_l X_1^{ij,kl}) + k_{ct} \sum_i \sum_j Y_1^{ij}([P_0\dot{T}P_0] \sum_i \sum_j T_0^{ij} + \sum_i \sum_j \sum_k \sum_l X_0^{ij,kl})]$
second-order moments	propagating radical chains	$\frac{dY_2^{ij}}{dt} = 4k_{p,ij}[P_{1,i}^\bullet][M_j] + \sum_k k_{p,kij}[M_j]Y_0^{ki} + 2\sum_k k_{p,kij}[M_j]Y_1^{ki} + \sum_k k_{p,kij}[M_j]Y_2^{ki} - \sum_k k_{p,ijk}[M_k]Y_2^{ij} - k_{a,j}Y_2^{ij}([TP_0] + \sum_k \sum_l Z_0^{kl}) + \frac{1}{2}k_{f,j}(T_2^{ij} + \sum_{k\neq i} \sum_{or\, l\neq j} X_{2,0}^{ij,kl} + \sum_{k=i} \sum_{l=j} X_2^{ij,kl}) - \{k_{tc,0}[P_0^\bullet] + \sum_k \sum_l (k_{tc,jl} + k_{td,jl})Y_0^{kl}\}Y_2^{ij} - k_{ct}Y_2^{ij}([P_0\dot{T}P_0] + \sum_k \sum_l T_0^{kl} + \sum_k \sum_l \sum_m \sum_n X_0^{kl,mn})$
	dormant chain	$\frac{dZ_2^{ij}}{dt} = \frac{1}{2}(k_{f,0}T_2^{ij} + \sum_k \sum_l k_{f,kl}X_{2,0}^{ij,kl}) - (k_{a,0}[P_0^\bullet] + \sum_k \sum_l k_{a,l}Y_0^{kl})Z_2^{ij}$
	primary intermediate radical chains	$\frac{dT_2^{ij}}{dt} = k_{a,0}[P_0^\bullet]Z_2^{ij} + k_{a,j}[TP_0]Y_2^{ij} - \frac{1}{2}(k_{f,0} + k_{f,j})T_2^{ij} - k_{ct}T_2^{ij}([P_0^\bullet] + \sum_k \sum_l Y_0^{kl})$
	intermediate radical chains	$\frac{dX_2^{ij,kl}}{dt} = k_{a,j}(Y_2^{ij}Z_0^{kl} + 2Y_1^{ij}Z_1^{kl} + Y_0^{ij}Z_2^{kl}) - k_{f,j}X_2^{ij,kl} - k_{ct}X_2^{ij,kl}([P_0^\bullet] + \sum_m \sum_n Y_0^{mn})$ $(i = k, j = l)$
		$\frac{dX_2^{ij,kl}}{dt} = k_{a,j}(Y_2^{ij}Z_0^{kl} + 2Y_1^{ij}Z_1^{kl} + Y_0^{ij}Z_2^{kl}) + k_{a,l}(Y_2^{kl}Z_0^{ij} + 2Y_1^{kl}Z_1^{ij} + Y_0^{kl}Z_2^{ij}) - \frac{1}{2}(k_{f,j} + k_{f,l})X_2^{ij,kl} - k_{ct}X_2^{ij,kl}([P_0^\bullet] + \sum_m \sum_n Y_0^{mn})$ $(i \neq k)$ or $(j \neq l)$
		$\frac{dX_{2,0}^{ij,kl}}{dt} = k_{a,j}Y_2^{ij}Z_0^{kl} + k_{a,l}Y_0^{ij}Z_2^{kl} - \frac{1}{2}(k_{f,j} + k_{f,l})X_{2,0}^{ij,kl} - k_{ct}X_{2,0}^{ij,kl}([P_0^\bullet] + \sum_m \sum_n Y_0^{mn})^a$
	dead chains	$\frac{dQ_2}{dt} = (k_{tc,0} + k_{td,0})[P_0^\bullet] \sum_i \sum_j Y_2^{ij} + \sum_i \sum_j \sum_k \sum_l k_{tc,jl}(Y_2^{ij}Y_0^{kl} + Y_1^{ij}Y_1^{kl}) + \sum_i \sum_j \sum_k \sum_l k_{td,jl}Y_2^{ij}Y_0^{kl} + k_{ct}[([P_0^\bullet] + \sum_i \sum_j Y_0^{ij})(\sum_i \sum_j T_2^{ij} + \sum_i \sum_j \sum_k \sum_l X_2^{ij,kl}) + k_{ct} \sum_i \sum_j Y_2^{ij}([P_0\dot{T}P_0] + \sum_i \sum_j T_0^{ij} + \sum_i \sum_j \sum_k \sum_l X_0^{ij,kl}) + 2k_{ct} \sum_i \sum_j Y_1^{ij}(T_0^{ij} + \sum_i \sum_j \sum_k \sum_l X_1^{ij,kl})$
small molecules	initiator	$\frac{d[I]}{dt} = -k_d[I]$
	monomers	$\frac{d[M_i]}{dt} = -k_{in,i}[P_0^\bullet][M_i] - \sum_j k_{p,ji}[P_{1,j}^\bullet][M_i] - \sum_k \sum_j k_{p,kji}Y_0^{kj}[M_i]$
	primary propagating radical	$\frac{d[P_0^\bullet]}{dt} = 2fk_d[I] - \sum_i k_{in,i}[M_i][P_0^\bullet] - k_{a,0}[P_0^\bullet]([TP_0] + \sum_i [TP_{1,i}] + \sum_i \sum_j Z_0^{ij}) + \frac{1}{2}k_{f,0}(\sum_i [P_{1,i}\dot{T}P_0] + \sum_i \sum_j T_0^{ij}) + k_{f,0}[P_0\dot{T}P_0] - k_{tc,0}[P_0^\bullet](2[P_0^\bullet] + \sum_i [P_{1,i}^\bullet] + \sum_i \sum_j Y_0^{ij}) - k_{ct}[P_0^\bullet]([P_0\dot{T}P_0] + \sum_i [P_{1,i}\dot{T}P_0] + \sum_i \sum_j [P_{1,i}\dot{T}P_{1,j}] + \sum_i \sum_j T_0^{ij} + \sum_i \sum_j \sum_k T_0^{ijk} + \sum_i \sum_j \sum_k \sum_l X_0^{ij,kl})$
	primary RAFT agent	$\frac{d[TP_0]}{dt} = k_{f,0}[P_0\dot{T}P_0] + \frac{1}{2}\sum_i k_{f,i}([P_{1,i}\dot{T}P_0] + \sum_j T_0^{ji}) - k_{a,0}[P_0^\bullet][TP_0] + \sum_i k_{a,i}([P_{1,i}^\bullet][TP_0] + \sum_j T_0^{ji})$
	primary intermediate radical	$\frac{d[P_0\dot{T}P_0]}{dt} = k_{a,0}[P_0^\bullet][TP_0] - k_{f0}[P_0\dot{T}P_0] - k_{ct0}[P_0\dot{T}P_0]([P_0^\bullet] + \sum_i [P_{1,i}^\bullet] + \sum_i \sum_j Y_0^{ij})$

[a] These equations are necessary for closure of the differential equations.

Appendix A: Kinetic Model

The appendix shows the details of kinetic model equations for the RAFT copolymerization shown in Tables 6 and 7.

Appendix B: Kinetic Rate Constants and Physical and Transport Properties for St/BA Copolymerization

Table 8. Kinetic Rate Constants of the St/BA RAFT Polymerization Used in Simulation

parameters	description	values	ref
k_d (s^{-1})	decomposition rate constant	1.58×10^{15} exp(−15503/T)	42
k_{p11} (L/mol/s)	propagation rate constant of St	4.266×10^{7} exp(−3909.61/T)	43
k_{p22} (L/mol/s)	propagation rate constant of BA	7.37×10^{5} exp(−1156.90/T)	44
k_{tc11} (L/mol/s)	recombination termination rate constant of St	2.0×10^{10} exp(−1553.01/T)	45
k_{tc22} (L/mol/s)	recombination termination rate constant of BA	2.57×10^{8} exp(−292/T)	46
k_{td11} (L/mol/s)	disproportionation termination rate constant of St	0	47
k_{td22} (L/mol/s)	disproportionation termination rate constant of BA	0	48
k_{t12}, k_{t21} (L/mol/s)	cross termination rate parameter	$(k_{t11} \cdot k_{t22})^{1/2}$	49, 50
r_1	monomer reactivity ratio for St	0.723	51
r_2	monomer reactivity ratio for BA	0.189	51
s_1	radical reactivity ratio for St	1	24
s_2	radical reactivity ratio for BA	0.012	24

Table 9. Physical and Transport Properties for the St/BA RAFT Polymerization

parameters	values	ref
ρ_{m1} (g/cm^3)	$0.9193 - 6.65 \times 10^{-4}(T - 273.15)$	49
ρ_{m2} (g/cm^3)	$0.9211 - 1 \times 10^{-3}(T - 273.15)$	49
ρ_p (g/cm^3)	1.05	49
α_p (K^{-1})	$F_{n1}\alpha_{p1} + F_{n2}\alpha_{p2}$	48
α_{p1} (K^{-1})	4.5×10^{-4}	52
α_{p2} (K^{-1})	4.8×10^{-4}	53
α_{m1} (K^{-1})	6.2×10^{-4}	52
α_{m2} (K^{-1})	1.19×10^{-3}	53
α_s (K^{-1})	1.099×10^{-3}	54
T_{gm1} (K)	185.15	47
T_{gm2} (K)	185.15	53
T_{gS} (K)	115	55
T_{gp1} (K)	373	52
T_{gp2} (K)	218	53

References and Notes

(1) Hawker, C. J.; Bosman, A. W.; Harth, E. *Chem. Rev.* **2001**, *101*, 3661−3688.
(2) Matyjaszewski, K.; Xia, J. *Chem. Rev.* **2001**, *101*, 2921−2990.
(3) Kamigaito, M.; Ando, T.; Sawamto, M. *Chem. Rev.* **2001**, *101*, 3689−3746.
(4) Fukuda, T.; Goto, A.; Ohno, K. *Macromol. Rapid Commun.* **2000**, *21*, 151−165.
(5) Patten, T. E.; Matyjaszewski, K. *Adv. Mater.* **1998**, *12*, 901−905.
(6) Moad, G.; Rizzardo, E.; Solomon, D. H. *Macromolecules* **1982**, *15*, 909−914.
(7) Chong, Y. K.; Le, T. P. T.; Moad, G.; Rizzardo, E.; Thang, S. H. *Macromolecules* **1999**, *32*, 2071−2074.
(8) Kubo, K.; Goto, A.; Sato, K.; Kwak, Y.; Fukuda, T. *Polymer* **2005**, *46*, 9762−9768.
(9) Luo, Y.; Liu, X. Z. *J. Polym. Sci., Part A: Polym. Chem.* **2004**, *42*, 6248−6258.
(10) Matyjaszewski, K. *Macromolecules* **2002**, *35*, 6773−6781.
(11) Charleux, B.; Nicolas, J.; Guerret, O. *Macromolecules* **2005**, *38*, 5485−5492.
(12) Hu, Z. Q.; Zhang, Z. C. *Macromolecules* **2006**, *39*, 1384−1390.
(13) Davis, K. A.; Matyjaszewski, K. *Adv. Polym. Sci.* **2002**, *159*, 1−169.
(14) Avehart, S. V.; Matyjaszewski, K. *Macromolecules* **1999**, *32*, 2221−2231.
(15) Ziegler, M. J.; Matyjaszewski, K. *Macromolecules* **2001**, *34*, 415−424.
(16) Min, K.; Li, M.; Matyjaszewski, K. *J. Polym. Sci., Part A: Polym. Chem.* **2005**, *43*, 3616−3622.
(17) Matyjaszewski, K.; Ziegler, M. J.; Arehart, S. V.; Greszta, D.; Pakula, T. *J. Phys. Org. Chem.* **2000**, *13*, 775−786.
(18) Kim, J.; Michelle, M. M.; Sandoval, R. W.; Woo, D. J.; Torkelson, J. M. *Macromolecules* **2006**, *39*, 6152−6160.
(19) Matyjaszewski, K. *Prog. Polym. Sci.* **2005**, *30*, 858−875.
(20) Urretabizkaia, A.; Leiza, J. R.; Asua, J. M. *AIChE J.* **1994**, *40*, 1850−1864.
(21) De, Buruaga, I. S.; Echevarria, A.; Armitage, P. D.; De, La, Cal, J. C.; Leiza, J. R.; Asua, J. M. *AIChE J.* **1997**, *43*, 1069−1081.
(22) Raphael, A. M.; Vieira, C. S.; Lima, E. L.; Pinto, J. C. *Ind. Eng. Chem. Res.* **2002**, *41*, 2915−2930.
(23) Coote, M. L.; Davis, T. P. *Prog. Polym. Sci.* **1999**, *24*, 1217−1251.
(24) Davis, T. P.; O'Driscoll, K. F.; Piton, M. C.; Winnik, M. A. *Polym. Int.* **1991**, *24*, 65−70.
(25) Chiefari, J.; Chong, Y. K.; Ercole, F.; Krstina, J.; Jeffery, J.; Le, T. P. T.; Mayadunne, R. T. A.; Meijs, G. F.; Moad, C. L.; Moad, G.; Rizzardo, E.; Thang, S. H. *Macromolecules* **1998**, *31*, 5559−5562.
(26) Wang, R.; Luo, Y.; Li, B.; Sun, X.; Zhu, S. *Macromol. Theory Simul.* **2006**, *15*, 356−368.
(27) Wang, A. R.; Zhu, S. *Macromol. Theory Simul.* **2003**, *12*, 196−208.
(28) Gilbert, R. G. *Emulsion Polymerization: A Mechanistic Approach*; Academic: London, 1995.
(29) Noyes, R. M. In *Effects of Diffusion Rates on Chemical Kinetics*; Porter, G., Ed.; Pergamon: London, 1961.
(30) Marten, F. L.; Hamielec, A. E. *J. Appl. Polym. Sci.* **1982**, *27*, 489−505.
(31) Neogi, P. *Diffusion in Polymers*; Marcel Dekker: New York, 1996, p 143.
(32) Achilias, D. S.; Kiparissides, C. *J. Appl. Polym. Sci.* **1988**, *35*, 1303−1323.
(33) Suzuki, H. *Macromolecules* **1989**, *22*, 1380−1384.
(34) Barner-Kowollik, C.; Quinn, J. F.; Uyen, Nguyen, T. L.; Heuts, J. P. A.; Davis, T. P. *Macromolecules* **2001**, *34*, 7849−7857.
(35) Vana, P.; Davis, T. P.; Barner-Kowollik, C. *Macromol. Rapid Commun.* **2002**, *23*, 952−956.
(36) Chernikova, E.; Morozov, A.; Leonova, E.; Garina, E.; Golubev, V.; Bui, C.; Charleux, B. *Macromolecules* **2004**, *37*, 6329−6339.
(37) Kwak, Y.; Goto, A.; Fukata, T. *Macromolecules* **2004**, *37*, 1219−1225.
(38) Kwak, Y.; Goto, A.; Tsujii, Y.; Murata, Y.; Komatsu, K.; Fukuda, T. *Macromolecules* **2002**, *35*, 3026−3029.
(39) Barner-Kowollik, C.; Quinn, J. F.; Morsley, D. R.; Davis, T. P. *J. Polym. Sci., Part A: Polym. Chem.* **2001**, *39*, 1353−1365.
(40) Drache, M.; Schmidt-Naake, G.; Buback, M.; Vana, P. *Polymer* **2005**, *46*, 8483−8493.
(41) Luo, Y.; Wang, R.; Yang, L.; Yu, B.; Li, B.; Zhu, S. *Macromolecules* **2006**, *39*, 1328−1337.
(42) Brandrup, J.; Immergut, E.; Grulke, E., Eds. *Polymer Handbook*, 4th ed.; Wiley: New York, 1999.
(43) Buback, M.; Gilbert, R. G.; Hutchinson, R. A.; Klumperman, B.; Kuchta, F.; Manders, B. G.; O'Driscoll, K. F.; Russell, G. T.; Schweer, J. *Macromol. Chem. Phys.* **1995**, *196*, 3267−3280.
(44) Beuermann, S.; Paquet, D. A., Jr.; McMinn, J. H.; Hutchinson, R. A. *Macromolecules* **1996**, *29*, 4206−4215.
(45) Hui, A. W.; Hamiclec, A. E. *J Appl. Polym. Sci.* **1972**, *16*, 749−769.
(46) Li, D.; Grady, M. C. Hutchinson, R. A. *Ind. Eng. Chem. Res.* **2005**, *44*, 2506−2517.
(47) Keramopoulos, A.; Kiparissides, C. *Macromolecules* **2002**, *35*, 4155−4166.
(48) Keramopoulos, A.; Kiparissides, C. *J Appl. Polym. Sci.* **2003**, *88*, 161−176.
(49) Zhang, M.; Ray, W. H. *J Appl. Polym. Sci.* **2002**, *86*, 1630−1662.
(50) Walling, C. *J. Am. Chem. Soc.* **1949**, *71*, 1930−1935.
(51) Kostanski, L. K.; Hamielec, A. E. *Polymer* **1992**, *33*, 3706−3710.
(52) Soh, S. K.; Sundberg, D. C. *J Polym Sci., Polym. Chem. Ed.* **1982**, *20*, 1331−1344.
(53) Dube, M. A.; Rilling, K.; Penlidis, A. *J Appl. Polym. Sci.* **1991**, *43*, 2137−2145.
(54) Yao, Y.; Xie, T.; Gao, Y., Eds. *Handbook of Chemistry and Physics*; Shanghai Scientific and Technical Publishers: Shanghai, 1985.
(55) Fedors, R. F. *J Polym Sci., Polym. Lett. Ed.* **1979**, *17*, 719−722.

MA061677V